Biochemical Society Transactions (2024) **52** 1647–1659
https://doi.org/10.1042/BST20230947

Review Article

Plant supercomplex I + III_2 structure and function: implications for the growing field

Maria Maldonado

Department of Plant Biology, University of California, Davis, Davis, CA, U.S.A.

Correspondence: Maria Maldonado (mmaldo@ucdavis.edu)

Mitochondrial respiration is major source of chemical energy for all free-living eukaryotes. Nevertheless, the mechanisms of the respiratory complexes and supercomplexes remain poorly understood. Here, I review recent structural and functional investigations of plant supercomplex I + III_2 from *Arabidopsis thaliana* and *Vigna radiata*. I discuss commonalities, open questions and implications for complex I, complex III_2 and supercomplexes in plants and non-plants. Studies across further clades will enhance our understanding of respiration and the potential universal mechanisms of its complexes and supercomplexes.

Introduction

The mitochondrial electron transport chain (mETC) couples the transfer of electrons from NADH and succinate to molecular oxygen to the pumping of protons across the inner mitochondrial membrane, from the mitochondrial matrix into the inter-membrane space (IMS). This generates an electrochemical proton gradient that is then used by ATP synthase to generate ATP for the cell. The mETC is composed of four multi-subunit membrane complexes (complex I–IV, CI–IV) as well as electron carriers quinone (in the membrane) and cytochrome *c* (in the IMS) [1]. While this canonical respiratory chain is present across free-living eukaryotes, plants (and other organisms) also contain an alternative respiratory chain that transfers electrons from NADH to oxygen via quinone without proton pumping [2]. Thus, although the alternative chain does not directly contribute to the proton gradient, it does affect mitochondrial NADH and quinone levels.

The canonical mETC complexes can exist in isolation or assemble into higher-order supercomplexes. Biochemical and *in situ* electron tomography studies suggest that supercomplexes may be the most abundant and physiologically relevant form of the mETC [3–5], although the advantages of assembling supercomplexes remains poorly understood. In plants, the most abundant supercomplex is the assembly between CI and $CIII_2$, i.e. supercomplex I + III_2 (SC I + III_2), containing 50–90% of CI [4,6]. Plant CI is a 48-subunit complex with 14 core subunits with catalytic roles and 34 accessory subunits with incompletely understood assembly, stability, or regulatory roles [3,7–9] (Figure 1a,b). The subunits are arranged into multiple modules that form a membrane arm (embedded in the inner mitochondrial membrane) and a peripheral arm that protrudes into the matrix (Figure 1c). The peripheral arm contains redox active sites in the N module (where NADH binds) and a Q module (where quinone binds). The membrane arm contains the proton pumps arranged in a proximal (P_P) and distal (P_D) module, as well as a γ-carbonic anhydrase (γCA) domain attached on the end of the P_P. Additionally, a more recently discovered bridge domain links plant CI's arms [9] (Figure 1c,d). The γCA and bridge domain are inferred to be ancestral domains present in the last eukaryotic common ancestor and lost in CI of mammals and fungi [10,11]. Plant $CIII_2$ is a 20-subunit obligate dimer (10 subunits per protomer) composed of a membrane domain (where electron transfer occurs) and a matrix domain composed of subunits of the mitochondrial processing peptidase (MPP) family [12] (Figure 1e). In plants, $CIII_2$'s MPP domain is active and provides the MPP activity that cleaves

Received: 6 May 2024
Revised: 1 August 2024
Accepted: 7 August 2024

Version of Record published: 23 August 2024

Biochemical Society Transactions (2024) **52** 1647–1659
https://doi.org/10.1042/BST20230947

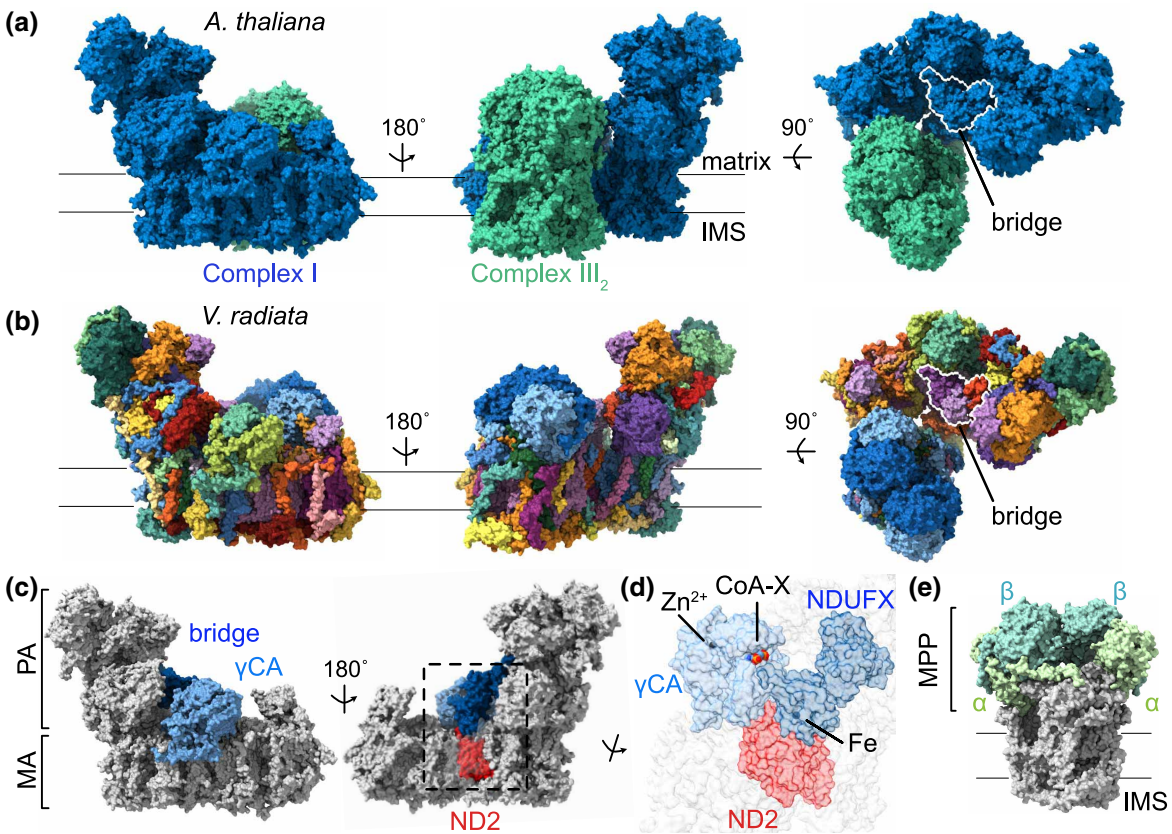

Figure 1. Structures of plant supercomplex (SC) I + III$_2$.

(**a**,**b**) CryoEM structure of SC I + III$_2$ from *A. thaliana* ([7], PDB: 8BPX) (**a**) and *V. radiata* ([8], PDB: 8E73) (**b**) in different orientations. Bridge domain in white silhouette in right panels. Approximate location of inner mitochondrial membrane shown. IMS, inter-membrane space. (**a**) Complex I in blue surface, complex III$_2$ in blue surface. (**b**) Complex I and complex III$_2$ colored by subunit, in surface representation. (**c**) Subunits involved in new hypothesized bioenergetic roles of γCA domain. γCA domain in light blue surface, bridge domain in dark blue surface, ND2 subunit in red surface, rest of complex I in gray surface. Note that NDUA11 and C-terminus of ND5 area shown semi-transparent to allow visualization of ND2. Dashed area is enlarged in (**d**). Approximate locations of the membrane arm (MA) and peripheral arm (PA) are indicated. (**d**) Detail of subunits and co-factors in dashed area in (**c**). Subunits in same color scheme as (**c**), with added transparency. CoA-X, crotonyl-CoA or butyryl-CoA. (**e**) Complex III$_2$ structure from SC I + III$_2$ (*V. radiata*) showing location of MPP domain. MPPα (α) in light green surface, MPPβ (β) in darker green surface.

the import signal from most proteins that are imported into the mitochondria [13–17]. Thus, in plants, CIII$_2$ is a dual respiratory and peptidase enzyme.

The mechanistic study of mETC complexes and supercomplexes is an active area of research across organisms. In this article, I review recent structural and functional investigations of plant SC I + III$_2$ from *Arabidopsis thaliana* [7] and *Vigna radiata* [8] (mung bean). I summarize key results from each paper and then discuss commonalities, differences, open questions and implications for CI and supercomplex mechanisms in plants and in non-plant organisms. I focus on CI's γCA anhydrase and bridge domains, catalytic loops and active-to-deactive transition, as well as on CIII$_2$'s MPP isoforms, and then discuss studies on the roles of supercomplexes.

Key findings for plant SC I + III$_2$

The structural and functional studies of SC I + III$_2$ from *A. thaliana* and *V. radiata* were published simultaneously [7,8]; data had not been exchanged between the groups before publication, to maximize the independence of the studies. The cryo-electron microscopy (cryoEM) structures of these plant SC I + III$_2$ are generally in

excellent agreement, particularly for CI and the supercomplex interfaces (Figure 1). In both structures, the binding of $CIII_2$ to CI's membrane arm led to the stabilization of and improved cryoEM densities for this region. This allowed for the identification of NDUP9 (a newly identified plant-specific subunit of CI), the modeling of previously missing segments of core subunits (e.g. ND5, ND6), as well as the retention and modeling of subunit NDUA11, which was missing in all previous plant CI structures. Thus, both structures provided the full complement of CI subunits (48) as well as the specific protein:protein interactions between CI and $CIII_2$. Three interfaces were observed: one in the mitochondrial matrix between NDUB9 from CI and MPP-α and MPP-β from $CIII_2$, one in the IMS between NDUP9 and NDUA11 from CI and QCR6 from $CIII_2$, and one in the transmembrane region between NDUA11 from CI and QCR8 from $CIII_2$. The bridge domain does not form part of any supercomplex interface. Both groups also observed a decreased flexibility between the matrix and membrane/IMS regions of $CIII_2$, in contrast to that previously seen in free *V. radiata* $CIII_2$ [12].

In their study, Klusch and team investigated the structure of SC I + III_2 from an *A. thaliana* cell suspension culture and obtained a 2.1 Å resolution structure [7]. This high resolution allowed for the modelling of ∼3000 well-ordered water molecules within the region of CI's central axis, E-channel and ubiquitin-binding channel (PDB: 8BPX). Well-ordered water molecules are relevant for CI because they provide the medium for proton conductance via hydrogen-bonded networks (Grotthus mechanism) [18]. As such, they play an essential role in CI's redox-coupled proton pumping mechanism from the matrix into the IMS, which remains incompletely understood [19–21]. The structure identified three potential proton entrances from the matrix into CI's central aqueous passage (the central channel) at core subunits ND2, ND4 and ND5 in the membrane arm. It also identified two potential proton exits into the IMS at ND2 and ND5. Within CI's γCA domain, the high-resolution structure revealed a water molecule in tetrahedral coordination by the Zn^{+2} atom between γCA1 and γCA2, confirming the plant γCA domain as a member of the CamH subclass and further suggesting the domain is catalytically active (yet to be confirmed experimentally). The structure also allowed for the assignment of a density between subunits γCA2 and γCAL-2 as butyryl- or crotonyl-CoA (CoA-X, the only undiscernible difference being a single or a double bond) (Figure 1d). This potential new active site has implications for a possible carbon-assimilation role for plant CI.

In our study, we obtained an overall 3.3 Å structure of SC I + III_2 from etiolated *V. radiata* hypocotyls [8]. Whereas the water molecules seen in *A. thaliana* were not observable in the *V. radiata* structure due to its lower overall resolution, density consistent with CoA-X is present in the *V. radiata* reconstructions but was not modeled due to insufficient resolution [8,22]. In the *V. radiata* SC I + III_2 structure, we observed differences in the $CIII_2$ isoforms found within SC I + III_2 compared to free $CIII_2$ and to $CIII_2$ in a supercomplex with complex IV (SC III_2 + IV, [12]). For CI, we examined the conformations of several catalytically relevant loops in the vicinity of the quinone-binding channel (ND1 TMH5–6, NDUFS2 β1–2, NDUFS7 α1–2 and α2–β1) and at the interface between CI's arms (Nad3 TMH2–3, Nad6 TMH3–4). Broadly speaking, these loops have been seen to be ordered in closed and active turnover states of CI and disordered in open and deactive states of CI from mammals, yeast and bacteria. Whether the different conformations of these loops represent active and deactive states of CI or different points in the catalytic cycle remains actively debated [19,20]. Most of the loops in *V. radiata* were disordered or in a mixed or intermediate state between those previously seen in other organisms, without neatly aligning with any one single state. The presence of a π-bulge in ND6's transmembrane helix 6 (TMH6) suggested our structure was in a resting state, consistent with its purification in the absence of substrate. Therefore, we concluded that resting conformation of the quinone-binding site of plant CI adopts a more ordered conformation than mammalian deactive CI. We also investigated the existence of a potential 'active-to-deactive' (A/D) transition in plant CI. This mechanism, observed in mammals and other vertebrates [23–25], is a transition that places CI in an off-pathway conformation in the absence of substrate. Similar to the intermediate state observed with the key loops, our functional results showed that *V. radiata* CI displays some but not all features of the A/D transition (susceptibility to NEM, but no change in susceptibility upon thermal deactivation or substrate pre-activation).

Implications and open questions

Carbonic anhydrase domain

Carbonic anhydrases catalyze the conversion of CO_2 and H_2O into HCO_3^- and a proton (H^+) via a catalytic Zn^{2+} ion. Based on the geometry of the putative active site between γCA1 and γCA2 (three histidine residues and an ordered water molecule coordinating a Zn^{2+} in tetrahedral geometry, as seen in the high-resolution SC

Biochemical Society Transactions (2024) **52** 1647–1659
https://doi.org/10.1042/BST20230947

$I + III_2$ structure of *A. thaliana*), it has been assumed that plant CI's γCA domain is catalytically active [7,26]. Moreover, it is hypothesized that the γCA hydration of CO_2 into HCO_3^- contributes to the refixation of carbon in the Calvin-Benson–Bassham cycle of photosynthesis in plants [27–30]. This is in line with the Zn^{2+} catalytic site being absent in *Polytomella* (non-photosynthetic green alga) [9], *Tetrahymena thermophila* (non-photosynthetic alveolate) [10] and *Euglena gracilis* (mixotrophic euglenid) [11] (Table 1). The finding of the CoA-X ligand in the γCA domain and the hydrated half-channel on the matrix side of ND2 (the core subunit to which the γCA domain is anchored, Figure 1c) in the recent *A. thaliana* SC $I + III_2$ structure [7] add layers to the hypothesized bioenergetic roles of the γCA domain (Figure 1d).

Crotonyl-CoA

First, given crotonyl-CoA's interactions with CO_2 in the carboxylation reaction of crotonyl-CoA carboxylase/reductase [32], it is now hypothesized that this co-factor helps position the CO_2 molecule to enable γCA's reaction in plants [7,26]. This is in line with density consistent with CoA-X being present in the *A. thaliana*, *V. radiata* and cauliflower CI structures [7–9, 22, 33] — although not previously assigned due to insufficient resolution — and absent in the CI γCA domain of *T. thermophila*, a non-photosynthetic alveolate [10]. A density consistent with CoA-X is also present in *Polytomella* sp., perhaps as a vestigial remnant [9,26]. No relevant density is present in mixotrophic organism *E. gracilis*, implying that the crotonyl-CoA connection is either only present in the green lineage, or only in purely photosynthetic organisms (photoautotrophs) rather than in mixotrophs (Table 1). Interestingly, *E. gracilis* shows a phosphoethanolamine phospholipid at the interface equivalent to CAL-2 and γCA1, suggesting that the interfaces between γCA subunits may be prone to binding hydrophobic molecules. Nevertheless, *E. gracilis* CI does have a different connection to crotonyl-CoA: it contains a new fatty acid synthesis (FAS) domain with homologs to NADH-dependent trans-2-enoyl-coenzyme A/acyl-carrier-protein reductases, which can reduce crotonyl-CoA into butyryl-CoA during mitochondrial anaerobic wax fermentation [34,35]. Although the enzymatic activity of this domain has not been shown yet, it does suggest a wider (more ancient) potentially direct relationship between CI and crotonyl-CoA, as well as between oxidative phosphorylation and FAS.

The molecular details of the putative new plant CoA-X/CO_2 active site, how it compares to crotonyl-CoA carboxylase/reductases [32], and how the CO_2 in this site would be transferred to the carbonic anhydrase Zn^{+2}-binding site have not been determined. We propose another non-mutually exclusive role for the CoA-X co-factor. CoA-X may be required for the assembly and integrity of the γCA domain, an early essential step in the assembly of the entire CI [36–41]. Linking CI assembly to the availability of crotonyl/butyryl-CoA may be a way to regulate the abundance of CI — and electron transfer through the canonical mETC — by the status of amino acid and fatty acid metabolism in different tissues or developmental stages [42]. For instance, this CoA-X 'sensor' would be particularly important during germination, where both high levels of CI assembly

Table 1. Comparison of features in the vicinity of the γ-carbonic anhydrase domain in various organisms whose structures have been determined

Species	Classification	Photosynthetic	Catalytic Zn in γCA	CoA-X density	Fe in FX	ND2 half-hannel	Ref.
Arabidopsis thaliana	Vascular plant	Yes	Yes	Yes	Fe (3 cys, 1 his)	Yes	[7]
Vigna radiata	Vascular plant	Yes	Yes	Likely	Fe (3 cys, 1 his)	N.D.	[8]
Polytomella	Green alga	No	No	Likely	No (lacks all four metal-binding amino acids)	N.D.	[9]
Euglena gracilis	Euglenid	Yes (mixotrophic)	No	No (phospho-ethanol-amine in similar location)	No (truncated FX fold)	N.D.	[11]
Tetrahymena thermophila	Alveolate	No	No	No	2Fe2S (4 cys)	N.D.	[10]
Thermosynechococcus elongatus	Cyanobacteria	Yes	N.A. (different CA)	N.A.	N.A.	N.D.	[31]

γCA, gamma-carbonic anhydrase domain; CoA-X, crotonyl-CoA or butyryl-Co-A; FX, ferredoxin subunit of CI; N.A., not applicable; N.D. not determined. For simplicity, classification is provided at familiar phylogenetic levels.

[38] and high levels of crotonyl/butyryl-coA from amino acid and fatty acid catabolism [42] are expected. This is in line with the increasingly appreciated roles of FAS in mitochondrial biogenesis and oxidative metabolism [43,44]. A re-examination and further testing of existing plant γCA deletion and point mutants [30,39,45–50] in light of the now known γCA domain composition, and the creation of further point mutants lacking the CoA-X binding sites will shed light on these hypotheses.

Proton (H^+) pumping at ND2

Second, the γCA functional hypothesis now also includes the H^+ that is produced by the CO_2 hydration reaction [26]. It is hypothesized that these protons generate a local gradient that facilitates H^+ entry into the matrix half-channel on ND2 (Figure 1c,d); proton entry would also be facilitated by electrostatic repulsion from the nearby Fe cation in the ferredoxin subunit of CI's bridge domain (NDUFX, see below) (Figure 1c,d). The ND2 half-channel identified in the *A. thaliana* SC I + III_2 was not seen in other recent high-resolution structures of CI from heterotrophic organisms [51–57]. However, this may be due to the 'snapshot' nature of cryoEM data collection, particularly from CI samples without substrate, as excellently discussed elsewhere [21]. Moreover, whereas NDUFX likely contains a Fe ion in vascular plants [9,58], it contains a 2Fe2S co-factor in *T. thermophila* [10] (non-photosynthetic) and no co-factor in *Polytomella* [9] (non-photosynthetic). In *E. gracilis* (mixotrophic), NDUFX has a truncated ferredoxin fold that is lacking the co-factor-coordinating elements altogether [11] (Table 1). Therefore, the question remains whether the ND2 half-channel is an underlying universal feature of CI's H^+ pumping mechanism or whether it is an adaptation of organisms with (presumed) γCA activity and Fe-containing co-factors in its vicinity (so far limited to vascular plants, given the *Polytomella* and *E. gracilis* findings).

Carbonic anhydrase activity in photosynthetic CI

In cyanobacteria, carbonic anhydrase activity is used as a carbon-concentrating mechanism to aid photosynthesis by certain versions of photosynthetic complexes evolutionarily related to CI (photosynthetic CI, PS-CI, a.k.a. NDH-1) [59,60]. PS-CI contains homologs of CI subunits in the membrane arm and Q module but lack the N module. Thus, these complexes use ferredoxin (rather than NADH) as the electron donor to quinone and couple this redox reaction to proton pumping across the membrane [61–64]. What can these PS-CI teach us about carbonic anhydrase and proton pumping activity in respiratory CI? In the carbon-concentrating PS-CIs studied so far [31], the reaction is carried out by a Zn^{2+}-binding protein (CupA) that is on the 'end' of PS-CI's membrane arm (rather than anchored to the ND2 homolog) and that is *not* related to canonical, multimeric α, β or γ carbonic anhydrases. Therefore, the potential carbonic anhydrase activity of respiratory CI might be an example of convergent evolution. In terms of proton pumping, although it is commonly assumed that PS-CI pumps protons through half-channels in membrane arm, including through the ND2 homolog, this has only been inferred from nearby arrangement of protonatable residues [65–67] or molecular dynamics simulations [31] rather than from the observation of Grotthus-competent ordered water molecules in high-resolution structures of PS-CI. Thus, further structural and functional work on PS-CI is needed. If an ND2-like proton pathway were present in PS-CI, it would predict its universal presence in respiratory CI as well. Moreover, if the ND2 half-channel were universal in all CIs, this would open additional mechanistic and evolutionary questions regarding the proposed γCA-induced local proton gradient and repulsion by the bridge ferredoxin co-factor, as CI's γCA and bridge domains are believed to have been present in the last eukaryotic common ancestor [10,26,68].

Determining the γCA activity, proton pathways and pumping mechanism(s) of CI and evolutionarily related complexes such as PS-CI in a variety of photosynthetic, mixotrophic and heterotrophic organisms is critical to understand how the enzyme works and whether it indeed has a universal mechanism.

Bridge domain

The existence of a bridge domain that links CI's membrane and peripheral arms was initially discovered in *A. thaliana* and *Polytomella* sp. [9]. In plants, the bridge domain is formed by subunit NDUA6 (B14) connected to the peripheral arm, acyl-carrier-protein subunit NDUAB1α (SDAP2) and NDUFX, a ferredoxin-like subunit that binds ND2 (membrane arm) and γCAL-2 (γCA domain). A larger bridge was later seen in *T. thermophila* [10] and *E. gracilis* [11]. In the initial *A. thaliana* CI structural analysis [9], CI was found in different structural classes corresponding to 'closed' CI with a full bridge (with an inter-arm angle of 106°) or 'open' CI with a partial bridge (inter-arm angle of 112°). Given that at the time the inter-arm angle of CI was thought to hold biological significance, it was hypothesized that the bridge may have a regulatory role on CI's mechanism. The

Biochemical Society Transactions (2024) **52** 1647–1659
https://doi.org/10.1042/BST20230947

structures of plant SC I + III_2, together with findings in other organisms that the inter-arm angle of CI is not critical for function [10,56,57], have updated this view. Now, both groups have concluded that the bridge domain of CI has structural rather than regulatory roles. The bridge domain restricts the angles between the CI arms, as shown by the fact that the SC I + III_2 cryoEM particles are classified into a single class or very few highly similar classes with a narrow range of angles between the CI arms. Similar findings were seen for the bridge domains of *T. thermophila* [10] *and E. gracilis* [11]. The 'open' CI particles in the initial *A. thaliana* CI structure [9] had a partial bridge and were also lacking accessory subunit NDUA11. Similar 'bridge-less' CI was observed in *V. radiata*'s SC I + III_2. Here, the lack of the bridge domain was always accompanied with the lack of subunits (e.g. NDUA11) and/or the disordering of catalytically relevant regions (e.g. TMHs in ND5 and ND6). This is highly reminiscent of that seen in partially degraded samples of mammalian CI [54], suggesting that the bridge-less particles in plants correspond to non-functional CI that likely arises from detrimental interactions between the sample and the cryoEM grid.

Additional evidence for the roles of the bridge comes from functional studies of NDUFX knockout mutants in *A. thaliana* [58]. These bridge-less mutants contain intact CI but are not able to form SC I + III_2. Therefore, the bridge-less supercomplex particles observed in the cryoEM data are more likely degradation products than assembly intermediates. Moreover, the bridge-mutant studies suggest that the bridge plays a key role in the correct assembly of CI's membrane arm and, consequently, its interactions with $CIII_2$. This has led to the hypotheses that the roles of the bridge domain are to (1) correctly position the γCA domain to enable efficient assembly of CI's P_d domain onto CI* (the last plant CI assembly intermediate, which contains the N, Q and P_P modules and lacks the P_d domain [38]) and/or (2) properly place NDUA11 to allow for the necessary CI:$CIII_2$ interactions in SC I + III_2 [58]. It is important to note that the bridge-less CI in the NDUFX mutants is not equivalent to bridge-less CI in the SC I + III_2 studies: the first cannot bind to $CIII_2$ but contains NDUA11, whereas the second most likely represents a previously fully bridged CI in SC I + III_2 that subsequently lost its bridge and NDUA11. Thus, the bridge-less SC I + III_2 structures cannot be used to test the above hypotheses. Testing these hypotheses will require the structural examination of CI from bridge-less mutants [58].

Catalytic loops

The conformational state of several key CI loops around the quinone-binding site has garnered attention as a way to define the active/deactive state of CI and draw inferences on its catalytic cycle [19]. Close inspection of the key CI loops shows excellent agreement between the *A. thaliana* (PDB: 8BPX, 8BQ5, 8BQ6) and the *V. radiata* SC I + III_2 models (PDB: 8E73) for all loops except for the NDUS2 (49 kDa) β1–2 loop, which contains a key histidine residue that binds the quinone headgroup in the quinone-binding pocket [7,8]. Although the loop was fully disordered in *V. radiata* (similar to murine deactive CI (PDB: 6G72) [69]), it was ordered in *A. thaliana*. Here, the loop resembled (but did not fully match) the 'retracted' conformation seen in ovine closed CI (PDB: 6ZKO) [52] and yeast CI in turnover (active) conditions (PDB: 7O6Y) [53] (Figure 2). The differences between *V. radiata* and *A. thaliana* may be due to small sequence differences surrounding the loop (the loop itself is perfectly conserved across *V. radiata*, *A. thaliana*, *Mus musculus* and *Yarrowia lipolytica*) or to the different purification protocols used. Either way, the comparison further supports the finding that the quinone-binding site of the resting state of plant CI can adopt more ordered conformations than those typically seen in deactive mammalian CI (the ordered S2 loop was also seen in yeast deactive CI, PDB: 7O71, [53]). Moreover, the ordered NDUS2 loop in *A. thaliana* further shows that changes in CI's inter-arm angle are *not* required to organize the loops.

These plant findings, as well as more recent observations of ordered loops in *E. gracilis* CI in the absence of substrate [11], emphasize that different species and clades can have different conformations for their resting-state CI. Therefore, caution should be taken when extrapolating aspects of CI based on features seen in mammals. The observations from plants and other non-opisthokont organisms need be considered in proposals of the universal mechanism of CI. Alternatively, it is possible that the details of CI's mechanism are different in different eukaryotic supergroups. The structural characterization of a broader set of organisms will benefit our understanding of CI function.

Active to deactive transition

Similar to the finding that *V. radiata*'s and *A. thaliana*'s catalytic loops were in conformations that did not neatly align with findings from mammals or yeast, the *V. radiata* A/D assays also showed a 'non-canonical' behavior for plant CI. In this assay, CI is exposed to NEM a thiol reactant that modifies a cysteine residue in ND3's TMH1–2 loop, which is part of the quinone-binding site. In mammals, the cysteine is exposed in the

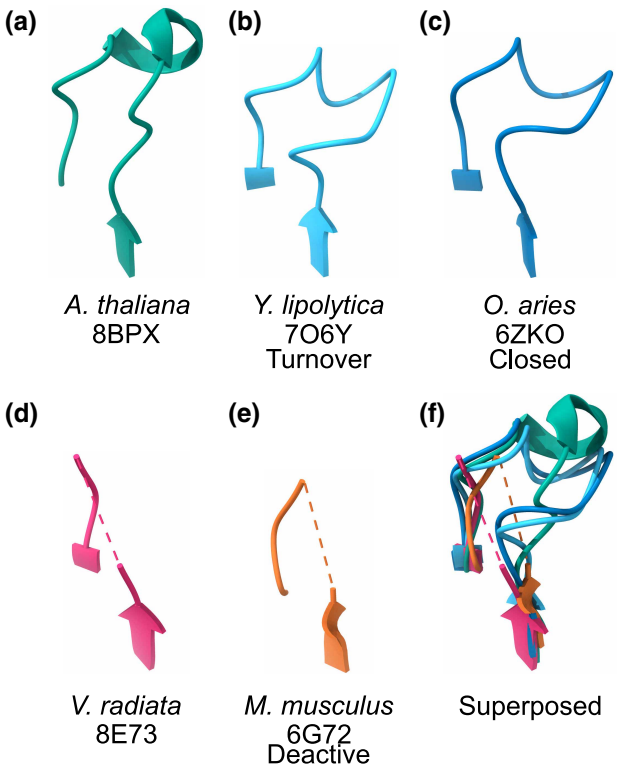

Figure 2. Differences in NDUS2 β1–2 loop model in different organisms and complex I (CI) states.

(**a**) *A. thaliana* CI within SC I + III_2 in the absence of substrate ([7], PDB: 8BPX). (**b**) *Y. lipolytica* CI in turnover conditions ([53], PDB: 7O6Y). (**c**) *O. aries* CI in closed conditions ([52], PDB: 6ZKO). (**d**) *V. radiata* CI within SC I + III_2 in the absence of substrate ([8], PDB: 8E73). (**e**) *M. musculus* CI in deactive conditions ([69], PDB: 6G72). (**f**) Superposition of (**a**–**e**).

deactive state and buried in the active/turnover state. Modification by NEM prevents the loop from going into its active conformation, thereby blocking CI in a deactive state and reducing the overall NADH-quinone oxidoreductase rate [70,71]. In organisms with a classic A/D transition, NEM effects are increased when CI is exposed to high temperature (37°C, thermal deactivation) and minimized when CI is pre-exposed to a low amount of NADH to put the enzyme in turnover conditions (pre-activation) [23]. Whereas *V. radiata* CI does show sensitivity to NEM, the sensitivity does not deepen with thermal deactivation and it does not lessen upon pre-activation [8]. This suggests that CI's active and deactive states are not biochemically distinct in plants as in mammals, but rather closer to each other. Likely, the active state conformation — in particular, the ordering of the ND3 TMH2–1 loop — is more accessible in the absence of substrate in plants than in other organisms (and/or the deactive state may also be more accessible in the presence of substrate). That is, the A/D functional assay also points to plant CI being capable of partial loop ordering in the resting state, in line with that seen in the *V. radiata* and *A. thaliana* structures.

Questions remain as to whether the presence of the bridge is what causes this A/D behavior, or whether it is mere correlation. The other organisms with a bridge in which the A/D transition was tested are *T. thermophila* and *E. gracilis*. In *T. thermophila*, the A/D transition is absent, with no effect of NEM on NADH oxidation rates [10]. In *E. gracilis*, very similar results to *V. radiata* were obtained: CI is sensitive to NEM, but this sensitivity is unaffected by NADH pre-activation (the effect of thermal deactivation was not examined) [11]. The A/D transition has also been examined in *Drosophila melanogaster* [72]. Although this organism does not have a bridge, it also shows a 'non-canonical' A/D behavior of a different kind: CI does show a lag phase in its activation when substrate is re-introduced (suggesting that *D. melanogaster* CI does go into an off-pathway resting state), but the activation is insensitive to the presence of NEM. This behavior correlates with a novel helix in NDUFS4 and a novel conformation for the C-terminal loop of NDUFA9 that lock the CI arms and hold several quinone-binding-site loops under a 'latch' [72]. These structural features may be part of a regulatory mechanism controlling the transitions between the CI active and resting states [72]. Together, this growing

Biochemical Society Transactions (2024) **52** 1647–1659
https://doi.org/10.1042/BST20230947

evidence suggests that the A/D transition may not be a binary feature of CI (absence/presence) and/or that the path from active to deactive may be differently traversed and regulated in different organisms. Therefore, studies of CI structure and A/D transition in as many and as biodiverse organisms as possible are needed.

When the quinone pool is over-reduced and the protonmotive force is high (high quinol/quinone and NAD^+/NADH ratios), there might be sufficient thermodynamic force to allow reverse electron transfer (RET) from quinol to NAD^+ by CI. This would be detrimental, as it would lead to high levels of reactive oxygen species (ROS). To prevent this, mammalian CI undergoes deactivation [70,73]. It was recently shown in a reconstituted system that deactive CI is *not* able to perform RET [74], confirming the protective nature of the A/D transition in mammals. It is currently unknown whether plant CI is capable of RET and whether a deactivation-like behavior of plant CI may protect against it. We previously hypothesized that the presence of the alternative oxidative phosphorylation chain in plants likely pushes CI closer to a RET regime (high quinol/quinone, high NAD^+/NADH ratios, see [22] Appendix 1) and that, therefore, a protective deactivation mechanism for CI is expected [22]. Yeast also contain an alternative oxidative phosphorylation chain with NDH and AOX homologs [75]. Interestingly, whereas CI from yeast *Y. lipolytica* is incapable of RET, CI from yeast *Pichia pastoris* performs RET at rates indistinguishable from those of bovine CI [74]. The inability of *Y. lipolytica* CI to perform RET is likely related to is tendency to easily enter the deactive state, as seen in functional and structural studies [23,51]. These differences suggest that the relationships between the presence of an alternative chain and CI structure and A/D dynamics will require careful examination. It is critical to determine the RET capabilities of plant CI in the active and deactive states, whether plant CI displays novel structural mechanisms for deactivation and how the activity of the alternative respiratory chain affects these issues.

$CIII_2$ subunits, activity and supercomplex assemblies

In *V. radiata*'s SC I + III_2 structure, we observed differences in the MPP-α isoforms present in the $CIII_2$ protomers. The protomer closest to CI corresponded to gene *LOC106765382*, which is different from *LOC106774328*, which we had previously observed in SC III_2 + IV and free $CIII_2$ from *V. radiata* [12]. The other protomer had more ambiguous density, with most positions more closely fitting *LOC106774328*, but some more closely resembling *LOC106765382*. Moreover, both protomers lacked their catalytic Zn^{2+} in MPP-β due partial disorder in the helix containing one of the coordinating residues (Glu217). Therefore, these structures correspond to a peptidase-inactive $CIII_2$. In contrast, both Zn^{2+} atoms had been visible in *V. radiata* SC III_2 + IV and free $CIII_2$ [12]. Although their peptidase activities were not tested, they are predicted to be active peptidases. Fittingly, $CIII_2$ exhibits significant conformational flexibility as a free complex or within SC III_2 + IV [12] but not within SC I + III_2 [7,8,12], likely due to the restraints imposed by the matrix interface with CI. Therefore, the current *V. radiata* structures suggest that $CIII_2$ may be an active peptidase in SC III_2 + IV or as an active complex, but not in SC I + III_2. In the *A. thaliana* SC I + III_2 structure both MPP-α isoforms were identical to each other, and both contained an ordered catalytic site in MPP-β with density for their coordinated Zn^{2+} (including a potentially coordinating water molecule), predicting an active $CIII_2$ in SC I + III_2. Atomic models for *A. thaliana* SC III_2 + IV or free $CIII_2$ are not available. Moreover, although *A. thaliana* contains two MPP-α isoforms, both exhibit higher sequence similarity to *V. radiata* LOC106774328 (isoform in SC III_2 + IV) than to *LOC106765382* (isoform in SC I + III_2). This inconclusive homology precludes straightforward inferences about *A. thaliana*'s MPP isoforms.

However, the *V. radiata* results raise multiple questions. Is $CIII_2$'s peptidase activity different in different supercomplex assemblies? If so, is the sorting based on the MPP isoforms? Are as-yet unidentified supercomplex assembly factors involved in differential sorting? Or is the isoform irrelevant and it is rather the interactions with CI that regulate MPP activity (e.g. MPP activity only from the MPP protomer not contacting CI)? Are there major differences between plant species? Support for the concept of differential sorting into separate supercomplexes comes from mammals, where, for instance, CI, $CIII_2$ and CIV can assemble into different respirasomes (C-MRC, S-MRC) based on the differential incorporation of COX7A isoforms [76] (see below). There is also some initial evidence for potential supercomplex assembly factors, although their existence remains unclear [77]. Answering these questions will require the functional, structural and complexome study of mutants of the various MPP-α and -β isoforms in multiple plant species.

Role of supercomplexes

The physiological roles of organizing the mETC into supercomplexes over having only individual complexes remain unclear. The fact that the available SC I + III_2 structures show interfaces involving different species-

specific details and subunits across four eukaryotic supergroups (mammals [78], alveolates [10], euglenids [11], plants [7,8] in Opisthokonta, TSAR, Excavata and Arachaeplastida, respectively) while sharing an overall similar location, orientation and architecture suggests that there is functional significance through convergent evolution [8,10]. What is the advantage of assembling respiratory complexes into supercomplexes?

Current hypotheses for the 'structural' role(s) of supercomplexes include to aid the assembly and stability of the individual complexes, to limit aggregation in the crowded environment of the cristae and to provide stoichiometric balance between complexes to prevent local differences in the quinol/quinone ratio thereby reducing ROS [79–81]. Evidence has been growing for a cooperative-assembly role for supercomplexes [77]. In this model, a key role of supercomplexes is to assist and promote the assembly and stabilization of the individual complexes. For instance, CI, $CIII_2$ and CIV assembly intermediates have been shown to associate in supercomplexes before (rather than after) the full assembly of the individual complexes [77]. There is also some initial evidence that supercomplex-specific assembly factors may exist to regulate the assembly of complexes via distinct supercomplex-first or individual complex-first biogenesis pathways [82,83].

Recent papers have also investigated the 'functional' consequences of an inability to form SC I + III_2. As discussed above, in *A. thaliana* the assembly of CI and $CIII_2$ into SC I + III_2 was almost completely disrupted by knocking out CI subunits NDUFX (in the bridge domain) or NDUA11 (interface subunit) [58]. The SC-less plants did not have phenotypes under the standard conditions assayed; however, stress conditions were not reported in that study. In mouse, the matrix interface (UQCRC1:NDUFB4) was disrupted by mutating three key residues on UQCRC1 (MPP-α) [84]. Conversely, the same interface was disrupted in human HEK293 T cells by mutating two key residues in NDUFB4 [85]. In both cases, the levels of CI-containing supercomplexes decreased ∼70–90%. With these low levels of SC I + III_2, under the conditions tested, the UQCRC1-mutated SC-less mice showed normal bioenergetic capacity (NADH oxidation, ROS production by CI, oxygen consumption rates, mitochondrial ATP production/oxygen consumption); in contrast, the NDUFB4-mutated SC-less human cells showed significantly reduced ATP-linked respiration and a compensatory shift toward succinate (CII)-linked respiration. From this contradiction, it is clear that further examination of the physiological effects of SC I + III_2 disruption under various conditions is needed.

Furthermore, it was recently shown that two SCI + III_2 + IV assemblies (C-MRC and S-MRC) with different isoforms of a CIV subunit (COX7A1/2 vs SCAFI) co-exist in human cells [76]. C-MRC vs S-MRC levels also vary in different human tissues [76]. CRISPR knockouts cells with only one type of the above supercomplexes showed the same respiratory rates but different net OXPHOS capacity, suggesting different abilities of C-MRC vs S-MRC to couple electron transfer to ATP synthesis. The authors also proposed that a metabolic shift from glycolytic to oxidative metabolism can reversibly regulate the relative abundance of C-MRC vs S-MRC [76]. Another recent paper investigated the roles of SC I + III_2 in *D. melanogaster* through a different approach. Fly mitochondria normally contain very low levels of SC I + III_2, likely owing to the truncation of NDUFB4's N-terminus [72,86]. Therefore, rather than assessing the consequences of disrupting supercomplexes, the study investigated the effect of increasing the level of SC I + III_2 by perturbing assembly factors of CI or $CIII_2$ or decreasing the levels of CI itself [87]. Mitochondria from flies with increased SC I + III_2 levels did not show respirometric differences from controls (beyond that from increases in protein levels of the individual complexes) or a preferential use of CI-linked electrons by $CIII_2$ (no increase in electron transfer efficiency between CI and $CIII_2$). Although this argues against a catalytic role for the organization into SC I + III_2, many questions remain — not least, whether *D. melanogaster* findings can be extrapolated to other organisms given that it does not normally form abundant supercomplexes.

Overall, given the different experimental settings and assays, as well as the contradictory results, it is too early to conclude that SC I + III_2, and respiratory supercomplexes in general, do not have roles 'beyond' structural ones. It is also possible that supercomplexes have different roles in different organisms and physiological settings. For instance, could supercomplexes be providing a kinetic advantage through complexes I–IV to regulate electron flow through the canonical vs alternative chains, in organisms like plants and fungi that possess both [88]? It also remains to be determined why there would exist regulatory supercomplex assembly factors (proposed to regulate the biogenesis of the OXPHOS complexes via supercomplexes or via individual complexes [77]), or regulated OXPHOS chain organizations into C- vs S-MRC supercomplexes (proposed to have different preponderance regulated by the extent of glycolytic vs oxidative metabolism [76]) if supercomplexes did not have catalytic roles. Why regulate something that provides no advantage?

The holy grail in the field seems to be to determine whether supercomplexes have a 'functional' (catalytic) role beyond 'merely structural' ones. Given that structural roles *are* functional roles, the functional vs structural

Biochemical Society Transactions (2024) **52** 1647–1659
https://doi.org/10.1042/BST20230947

differentiation may be a false dichotomy. For instance, even if the 'only' role of SCI $I + III_2$ were to promote proper and timely assembly of CI and $CIII_2$, this would be a significant functional role — regardless of whether the supercomplex organization also affected catalytic rates or the respiratory capacity of the cell.

Overall, studies, interpretations and proposed models for the functions and mechanisms of supercomplexes and the individual complexes should account for observations across the tree of life when proposing universal mechanisms and consider that functions may be different in different clades. Studies across further clades will enhance our understanding of the mechanisms of respiratory complexes and supercomplexes.

Perspectives

- Respiratory supercomplexes are the main physiological form of respiratory CI in plants (and other organisms), yet the roles of the supercomplexes and the mechanisms of the individual complexes remain incompletely understood.
- Recent structural and functional studies of plant supercomplex $I + III_2$ from two different species allow for further insight into CI, $CIII_2$ and supercomplexes by comparing to each other and to non-plant organisms.
- Many open questions remain. How does subunit composition diversity contribute to CI's assembly and regulation? What are CI's proton pumping pathways, and how conserved are they? Does CI's γCA domain contribute to proton pumping (in what organisms)? How does CI's bridge affect CI assembly, deactivation and supercomplex formation? Are CI's loop conformations related to its catalytic cycle or to its active-to-deactive transition? Should we re-conceptualize the active-to-deactive transition? Can plant CI carry out RET? If so, what is the relationship with deactivation and the alternative respiratory chain? Is plant $CIII_2$'s MPP domain active in supercomplexes? Do MPP isoforms lead to differential supercomplex sorting? Do supercomplexes affect respiratory function? Are supercomplex roles different in different clades?

Competing Interests

The author declares that there are no competing interests associated with this manuscript.

Open Access

Open access for this article was enabled by the participation of University of California in an all-inclusive *Read & Publish* agreement with Portland Press and the Biochemical Society under a transformative agreement with UC.

Acknowledgements

I thank James Letts, Hans-Peter Braun and reviewers for their helpful comments on the manuscript.

Abbreviations

γCA, γ-carbonic anhydrase; cryoEM, cryo-electron microscopy; IMS, inter-membrane space; mETC, mitochondrial electron transport chain; MPP, mitochondrial processing peptidase; RET, reverse electron transfer.

References

1 Nicholls, D.G. and Ferguson, S.J. (2013) *Bioenergetics 4*, Academic Press, London
2 Rasmusson, A.G., Geisler, D.A. and Moller, I.M. (2008) The multiplicity of dehydrogenases in the electron transport chain of plant mitochondria. *Mitochondrion* **8**, 47–60 https://doi.org/10.1016/j.mito.2007.10.004
3 Padavannil, A., Ayala-Hernandez, M.G., Castellanos-Silva, E.A. and Letts, J.A. (2021) The mysterious multitude: structural perspective on the accessory subunits of respiratory complex I. *Front. Mol. Biosci.* **8**, 798353 https://doi.org/10.3389/fmolb.2021.798353
4 Eubel, H., Heinemeyer, J. and Braun, H.P. (2004) Identification and characterization of respirasomes in potato mitochondria. *Plant Physiol.* **134**, 1450–1459 https://doi.org/10.1104/pp.103.038018

5 Davies, K.M., Blum, T.B. and Kuhlbrandt, W. (2018) Conserved in situ arrangement of complex I and III_2 in mitochondrial respiratory chain supercomplexes of mammals, yeast, and plants. *Proc. Natl Acad. Sci. U.S.A.* **115**, 3024–3029 https://doi.org/10.1073/pnas.1720702115
6 Eubel, H., Jansch, L. and Braun, H.P. (2003) New insights into the respiratory chain of plant mitochondria. Supercomplexes and a unique composition of complex II. *Plant Physiol.* **133**, 274–286 https://doi.org/10.1104/pp.103.024620
7 Klusch, N., Dreimann, M., Senkler, J., Rugen, N., Kühlbrandt, W. and Braun, H.-P. (2023) Cryo-EM structure of the respiratory I + III_2 supercomplex from *Arabidopsis thaliana* at 2Å resolution. *Nat. Plants* **9**, 142–156 https://doi.org/10.1038/s41477-022-01308-6
8 Maldonado, M., Fan, Z., Abe, K.M. and Letts, J.A. (2023) Plant-specific features of respiratory supercomplex I + III_2 from *Vigna radiata*. *Nat. Plants* **9**, 157–168 https://doi.org/10.1038/s41477-022-01306-8
9 Klusch, N., Senkler, J., Yildiz, O., Kuhlbrandt, W. and Braun, H.P. (2021) A ferredoxin bridge connects the two arms of plant mitochondrial complex I. *Plant Cell* **33**, 2072–2091 https://doi.org/10.1093/plcell/koab092
10 Zhou, L., Maldonado, M., Padavannil, A., Guo, F. and Letts, J.A. (2022) Structures of Tetrahymena's respiratory chain reveal the diversity of eukaryotic core metabolism. *Science* **376**, 831 https://doi.org/10.1126/science.abn7747
11 He, Z., Wu, M., Tian, H., Wang, L., Hu, Y., Han, F. et al. (2024) Euglena's atypical respiratory chain adapts to the discoidal cristae and flexible metabolism. *Nat. Commun.* **15**, 1628 https://doi.org/10.1038/s41467-024-46018-z
12 Maldonado, M., Guo, F. and Letts, J.A. (2021) Atomic structures of respiratory complex III_2, complex IV, and supercomplex III_2-IV from vascular plants. *eLife* **10**, e62047. https://doi.org/10.7554/eLife.62047
13 Braun, H.P., Emmermann, M., Kruft, V. and Schmitz, U.K. (1992) The general mitochondrial processing peptidase from potato is an integral part of cytochrome c reductase of the respiratory chain. *EMBO J.* **11**, 3219–3227 https://doi.org/10.1002/j.1460-2075.1992.tb05399.x
14 Braun, H.P. and Schmitz, U.K. (1992) Affinity purification of cytochrome c reductase from potato mitochondria. *Eur. J. Biochem.* **208**, 761–767 https://doi.org/10.1111/j.1432-1033.1992.tb17245.x
15 Emmermann, M., Braun, H.P., Arretz, M. and Schmitz, U.K. (1993) Characterization of the bifunctional cytochrome c reductase-processing peptidase complex from potato mitochondria. *J. Biol. Chem.* **268**, 18936–18942 https://doi.org/10.1016/S0021-9258(17)46717-2
16 Emmermann, M. and Schmitz, U.K. (1993) The cytochrome c reductase integrated processing peptidase from potato mitochondria belongs to a new class of metalloendoproteases. *Plant Physiol.* **103**, 615–620 https://doi.org/10.1104/pp.103.2.615
17 Eriksson, A., Sjoling, S. and Glaser, E. (1994) The ubiquinol cytochrome c oxidoreductase complex of spinach leaf mitochondria is involved in both respiration and protein processing. *Biochim. Biophys. Acta* **1186**, 221–231 https://doi.org/10.1016/0005-2728(94)90181-3
18 Popov, I., Zhu, Z., Young-Gonzales, A.R., Sacci, R.L., Mamontov, E., Gainaru, C. et al. (2023) Search for a Grotthuss mechanism through the observation of proton transfer. *Commun. Chem.* **6**, 1–10 https://doi.org/10.1038/s42004-023-00878-6
19 Chung, I.J., Grba, D.N., Wright, J.J. and Hirst, J. (2022) Making the leap from structure to mechanism: are the open states of mammalian complex I identified by cryoEM resting states or catalytic intermediates? *Curr. Opin. Struct. Biol.* **77**, 102447 https://doi.org/10.1016/j.sbi.2022.102447
20 Kampjut, D. and Sazanov, L.A. (2022) Structure of respiratory complex I - an emerging blueprint for the mechanism. *Curr. Opin. Struct. Biol.* **74**, 102350. https://doi.org/10.1016/j.sbi.2022.102350
21 Grba, D.N., Chung, I., Bridges, H.R., Agip, A.-N.A. and Hirst, J. (2023) Investigation of hydrated channels and proton pathways in a high-resolution cryo-EM structure of mammalian complex I. *Sci. Adv.* **9**, eadi1359 https://doi.org/10.1126/sciadv.adi1359
22 Maldonado, M., Padavannil, A., Zhou, L., Guo, F. and Letts, J.A. (2020) Atomic structure of a mitochondrial complex I intermediate from vascular plants. *eLife* **9**, e56664. https://doi.org/10.7554/eLife.56664
23 Maklashina, E., Kotlyar, A.B. and Cecchini, G. (2003) Active/de-active transition of respiratory complex I in bacteria, fungi, and animals. *Biochim. Biophys. Acta* **1606**, 95–103 https://doi.org/10.1016/s0005-2728(03)00087-2
24 Kotlyar, A.B. and Vinogradov, A.D. (1990) Slow active inactive transition of the mitochondrial Nadh-ubiquinone reductase. *Biochim. Biophys. Acta* **1019**, 151–158 https://doi.org/10.1016/0005-2728(90)90137-S
25 Babot, M., Birch, A., Labarbuta, P. and Galkin, A. (2014) Characterisation of the active/de-active transition of mitochondrial complex I. *Biochim. Biophys. Acta* **1837**, 1083–1092 https://doi.org/10.1016/j.bbabio.2014.02.018
26 Braun, H.-P. and Klusch, N. (2024) Promotion of oxidative phosphorylation by complex I-anchored carbonic anhydrases? *Trends Plant Sci.* **29**, 64–71 https://doi.org/10.1016/j.tplants.2023.07.007
27 Braun, H.-P. and Zabaleta, E. (2007) Carbonic anhydrase subunits of the mitochondrial NADH dehydrogenase complex (complex I) in plants. *Physiol. Plant* **129**, 114–122 https://doi.org/10.1111/j.1399-3054.2006.00773.x
28 Martin, V., Villarreal, F., Miras, I., Navaza, A., Haouz, A., Gonzalez-Lebrero, R.M. et al. (2009) Recombinant plant gamma carbonic anhydrase homotrimers bind inorganic carbon. *FEBS Lett.* **583**, 3425–3430 https://doi.org/10.1016/j.febslet.2009.09.055
29 Zabaleta, E., Martin, M.V. and Braun, H.P. (2012) A basal carbon concentrating mechanism in plants? *Plant Sci.* **187**, 97–104 https://doi.org/10.1016/j.plantsci.2012.02.001
30 Soto, D., Córdoba, J.P., Villarreal, F., Bartoli, C., Schmitz, J., Maurino, V.G. et al. (2015) Functional characterization of mutants affected in the carbonic anhydrase domain of the respiratory complex I in *Arabidopsis thaliana*. *Plant J.* **83**, 831–844 https://doi.org/10.1111/tpj.12930
31 Schuller, J.M., Saura, P., Thiemann, J., Schuller, S.K., Gamiz-Hernandez, A.P., Kurisu, G. et al. (2020) Redox-coupled proton pumping drives carbon concentration in the photosynthetic complex I. *Nat. Commun.* **11**, 494 https://doi.org/10.1038/s41467-020-14347-4
32 Stoffel, G.M.M., Saez, D.A., DeMirci, H., Vögeli, B., Rao, Y., Zarzycki, J. et al. (2019) Four amino acids define the CO2 binding pocket of enoyl-CoA carboxylases/reductases. *Proc. Natl Acad. Sci. U.S.A.* **116**, 13964–13969 https://doi.org/10.1073/pnas.1901471116
33 Soufari, H., Parrot, C., Kuhn, L., Waltz, F. and Hashem, Y. (2020) Specific features and assembly of the plant mitochondrial complex I revealed by cryo-EM. *Nat. Commun.* **11**, 5195 https://doi.org/10.1038/s41467-020-18814-w
34 Anaerobic respiration coupled with mitochondrial fatty acid synthesis in wax ester fermentation by *Euglena gracilis* - Nakazawa - 2018 - FEBS Letters - Wiley Online Library. n.d. https://febs.onlinelibrary.wiley.com/doi/full/10.1002/1873-3468.13276 (accessed March 20, 2024)
35 Airenne, T.T., Torkko, J.M., Van den plas, S., Sormunen, R.T., Kastaniotis, A.J., Wierenga, R.K. et al. (2003) Structure-function analysis of enoyl thioester reductase involved in mitochondrial maintenance. *J. Mol. Biol.* **327**, 47–59 https://doi.org/10.1016/s0022-2836(03)00038-x

36 Meyer, E.H., Solheim, C., Tanz, S.K., Bonnard, G. and Millar, A.H. (2011) Insights into the composition and assembly of the membrane arm of plant complex I through analysis of subcomplexes in Arabidopsis mutant lines. *J. Biol. Chem.* **286**, 26081–26092 https://doi.org/10.1074/jbc.M110.209601
37 Li, L., Nelson, C.J., Carrie, C., Gawryluk, R.M.R., Solheim, C., Gray, M.W. et al. (2013) Subcomplexes of ancestral respiratory complex I subunits rapidly turn over *in vivo* as productive assembly intermediates in *Arabidopsis*. *J. Biol. Chem.* **288**, 5707–5717 https://doi.org/10.1074/jbc.M112.432070
38 Ligas, J., Pineau, E., Bock, R., Huynen, M.A. and Meyer, E.H. (2019) The assembly pathway of complex I in *Arabidopsis thaliana*. *Plant J.* **97**, 447–459 https://doi.org/10.1111/tpj.14133
39 Fromm, S., Senkler, J., Zabaleta, E., Peterhansel, C. and Braun, H.P. (2016) The carbonic anhydrase domain of plant mitochondrial complex I. *Physiol. Plant* **157**, 289–296 https://doi.org/10.1111/ppl.12424
40 Senkler, J., Senkler, M. and Braun, H.P. (2017) Structure and function of complex I in animals and plants - a comparative view. *Physiol. Plant* **161**, 6–15 https://doi.org/10.1111/ppl.12561
41 Braun, H.P. (2020) The oxidative phosphorylation system of the mitochondria in plants. *Mitochondrion* **53**, 66–75 https://doi.org/10.1016/j.mito.2020.04.007
42 Hildebrandt, T.M., Nunes Nesi, A., Araújo, W.L. and Braun, H.-P. (2015) Amino acid catabolism in plants. *Mol. Plant* **8**, 1563–1579 https://doi.org/10.1016/j.molp.2015.09.005
43 Wedan, R.J., Longenecker, J.Z. and Nowinski, S.M. (2024) Mitochondrial fatty acid synthesis is an emergent central regulator of mammalian oxidative metabolism. *Cell Metab* **36**, 36–47 https://doi.org/10.1016/j.cmet.2023.11.017
44 Nowinski, S.M., Van Vranken, J.G., Dove, K.K. and Rutter, J. (2018) Mitochondrial fatty acid synthesis is the puppet master of mitochondrial biogenesis. *Curr. Biol.* **28**, R1212–R1219 https://doi.org/10.1016/j.cub.2018.08.022
45 Perales, M., Eubel, H., Heinemeyer, J., Colaneri, A., Zabaleta, E. and Braun, H.-P. (2005) Disruption of a nuclear gene encoding a mitochondrial gamma carbonic anhydrase reduces complex I and supercomplex I + III_2 levels and alters mitochondrial physiology in Arabidopsis. *J. Mol. Biol.* **350**, 263–277 https://doi.org/10.1016/j.jmb.2005.04.062
46 Cordoba, J.P., Fassolari, M., Marchetti, F., Soto, D., Pagnussat, G.C. and Zabaleta, E. (2019) Different types domains are present in complex I from immature seeds and of CA adult plants in *Arabidopsis thaliana*. *Plant Cell Physiol.* **60**, 986–998 https://doi.org/10.1093/pcp/pcz011
47 Fromm, S., Senkler, J., Eubel, H., Peterhänsel, C. and Braun, H.-P. (2016) Life without complex I: proteome analyses of an Arabidopsis mutant lacking the mitochondrial NADH dehydrogenase complex. *J. Exp. Bot.* **67**, 3079–3093 https://doi.org/10.1093/jxb/erw165
48 Fromm, S., Göing, J., Lorenz, C., Peterhänsel, C. and Braun, H.-P. (2016) Depletion of the "gamma-type carbonic anhydrase-like" subunits of complex I affects central mitochondrial metabolism in *Arabidopsis thaliana*. *Biochim. Biophys. Acta* **1857**, 60–71 https://doi.org/10.1016/j.bbabio.2015.10.006
49 Fromm, S., Braun, H.-P. and Peterhansel, C. (2016) Mitochondrial gamma carbonic anhydrases are required for complex I assembly and plant reproductive development. *New Phytol.* **211**, 194–207 https://doi.org/10.1111/nph.13886
50 Wang, Q., Fristedt, R., Yu, X., Chen, Z., Liu, H., Lee, Y. et al. (2012) The γ-carbonic anhydrase subcomplex of mitochondrial complex I is essential for development and important for photomorphogenesis of Arabidopsis. *Plant Physiol.* **160**, 1373–1383 https://doi.org/10.1104/pp.112.204339
51 Grba, D.N. and Hirst, J. (2020) Mitochondrial complex I structure reveals ordered water molecules for catalysis and proton translocation. *Nat. Struct. Mol. Biol.* **27**, 892 https://doi.org/10.1038/s41594-020-0473-x
52 Kampjut, D. and Sazanov, L.A. (2020) The coupling mechanism of mammalian respiratory complex I. *Science* **370**, 547 https://doi.org/10.1126/science.abc4209
53 Parey, K., Lasham, J., Mills, D.J., Djurabekova, A., Haapanen, O., Yoga, E.G. et al. (2021) High-resolution structure and dynamics of mitochondrial complex I-insights into the proton pumping mechanism. *Sci. Adv.* **7**, eabj3221 https://doi.org/10.1126/sciadv.abj3221
54 Chung, I., Wright, J.J., Bridges, H.R., Ivanov, B.S., Biner, O., Pereira, C.S. et al. (2022) Cryo-EM structures define ubiquinone-10 binding to mitochondrial complex I and conformational transitions accompanying Q-site occupancy. *Nat. Commun.* **13**, 2758 https://doi.org/10.1038/s41467-022-30506-1
55 Gu, J., Liu, T., Guo, R., Zhang, L. and Yang, M. (2022) The coupling mechanism of mammalian mitochondrial complex I. *Nat. Struct. Mol. Biol.* **29**, 172–182 https://doi.org/10.1038/s41594-022-00722-w
56 Kravchuk, V., Petrova, O., Kampjut, D., Wojciechowska-Bason, A., Breese, Z. and Sazanov, L. (2022) A universal coupling mechanism of respiratory complex I. *Nature* **609**, 808 https://doi.org/10.1038/s41586-022-05199-7
57 Laube, E., Meier-Credo, J., Langer, J.D. and Kühlbrandt, W. (2022) Conformational changes in mitochondrial complex I of the thermophilic eukaryote *Chaetomium thermophilum*. *Sci. Adv.* **8**, eadc9952 https://doi.org/10.1126/sciadv.adc9952
58 Röhricht, H., Przybyla-Toscano, J., Forner, J., Boussardon, C., Keech, O., Rouhier, N. et al. (2023) Mitochondrial ferredoxin-like is essential for forming complex I-containing supercomplexes in Arabidopsis. *Plant. Physiol.* **191**, 2170–2184 https://doi.org/10.1093/plphys/kiad040
59 Price, G.D., Maeda, S., Omata, T. and Badger, M.R. (2002) Modes of active inorganic carbon uptake in the cyanobacterium, Synechococcus sp. PCC7942. *Funct. Plant Biol.* **29**, 131 https://doi.org/10.1071/PP01229
60 Badger, M.R. and Price, G.D. (2003) CO_2 concentrating mechanisms in cyanobacteria: molecular components, their diversity and evolution. *J. Exp. Bot.* **54**, 609–622 https://doi.org/10.1093/jxb/erg076
61 Battchikova, N., Eisenhut, M. and Aro, E.-M. (2011) Cyanobacterial NDH-1 complexes: novel insights and remaining puzzles. *Biochim. Biophys. Acta* **1807**, 935–944 https://doi.org/10.1016/j.bbabio.2010.10.017
62 Peltier, G., Aro, E.-M. and Shikanai, T. (2016) NDH-1 and NDH-2 plastoquinone reductases in oxygenic photosynthesis. *Annu. Rev. Plant Biol.* **67**, 55–80 https://doi.org/10.1146/annurev-arplant-043014-114752
63 Brandt, U. (2019) Adaptations of an ancient modular machine. *Science* **363**, 230–231 https://doi.org/10.1126/science.aaw0493
64 Richardson, K.H., Wright, J.J., Šimėnas, M., Thiemann, J., Esteves, A.M., McGuire, G. et al. (2021) Functional basis of electron transport within photosynthetic complex I. *Nat. Commun.* **12**, 5387 https://doi.org/10.1038/s41467-021-25527-1
65 Laughlin, T.G., Bayne, A.N., Trempe, J.F., Savage, D.F. and Davies, K.M. (2019) Structure of the complex I-like molecule NDH of oxygenic photosynthesis. *Nature* **566**, 411–414 https://doi.org/10.1038/s41586-019-0921-0
66 Schuller, J.M., Birrell, J.A., Tanaka, H., Konuma, T., Wulfhorst, H., Cox, N. et al. (2019) Structural adaptations of photosynthetic complex I enable ferredoxin-dependent electron transfer. *Science* **363**, 257–260 https://doi.org/10.1126/science.aau3613

67 Zhang, C., Shuai, J., Ran, Z., Zhao, J., Wu, Z., Liao, R. et al. (2020) Structural insights into NDH-1 mediated cyclic electron transfer. *Nat. Commun.* **11**, 888 https://doi.org/10.1038/s41467-020-14732-z
68 Gawryluk, R.M. and Gray, M.W. (2010) Evidence for an early evolutionary emergence of gamma-type carbonic anhydrases as components of mitochondrial respiratory complex I. *BMC Evol. Biol.* **10**, 176 https://doi.org/10.1186/1471-2148-10-176
69 Agip, A.A., Blaza, J.N., Bridges, H.R., Viscomi, C., Rawson, S., Muench, S.P. et al. (2018) Cryo-EM structures of complex I from mouse heart mitochondria in two biochemically defined states. *Nat. Struct. Mol. Biol.* **25**, 548–556 https://doi.org/10.1038/s41594-018-0073-1
70 Chouchani, E.T., Methner, C., Nadtochiy, S.M., Logan, A., Pell, V.R., Ding, S. et al. (2013) Cardioprotection by S-nitrosation of a cysteine switch on mitochondrial complex I. *Nat. Med.* **19**, 753–759 https://doi.org/10.1038/nm.3212
71 Yin, Z., Burger, N., Kula-Alwar, D., Aksentijevic, D., Bridges, H.R., Prag, H.A. et al. (2021) Structural basis for a complex I mutation that blocks pathological ROS production. *Nat. Commun.* **12**, 707 https://doi.org/10.1038/s41467-021-20942-w
72 Padavannil, A., Murari, A., Rhooms, S.-K., Owusu-Ansah, E. and Letts, J.A. (2023) Resting mitochondrial complex I from *Drosophila melanogaster* adopts a helix-locked state. *eLife* **12**, e84415 https://doi.org/10.7554/eLife.84415
73 Chouchani, E.T., Pell, V.R., Gaude, E., Aksentijevic, D., Sundier, S.Y., Robb, E.L. et al. (2014) Ischaemic accumulation of succinate controls reperfusion injury through mitochondrial ROS. *Nature* **515**, 431 https://doi.org/10.1038/nature13909
74 Wright, J.J., Biner, O., Chung, I., Burger, N., Bridges, H.R. and Hirst, J. (2022) Reverse electron transfer by respiratory complex I catalyzed in a modular proteoliposome system. *J. Am. Chem. Soc.* **144**, 6791–6801 https://doi.org/10.1021/jacs.2c00274
75 Antos-Krzeminska, N. and Jarmuszkiewicz, W. (2019) Alternative type II NAD(P)H dehydrogenases in the mitochondria of protists and fungi. *Protist* **170**, 21–37 https://doi.org/10.1016/j.protis.2018.11.001
76 Fernández-Vizarra, E., López-Calcerrada, S., Sierra-Magro, A., Pérez-Pérez, R., Formosa, L.E., Hock, D.H. et al. (2022) Two independent respiratory chains adapt OXPHOS performance to glycolytic switch. *Cell Metab* **34**, 1792–1808.e6 https://doi.org/10.1016/j.cmet.2022.09.005
77 Fernandez-Vizarra, E. and Ugalde, C. (2022) Cooperative assembly of the mitochondrial respiratory chain. *Trends Biochem. Sci.* **47**, 999–1008 https://doi.org/10.1016/j.tibs.2022.07.005
78 Letts, J.A., Fiedorczuk, K., Degliesposti, G., Skehel, M. and Sazanov, L.A. (2019) Structures of respiratory supercomplex I + III_2 reveal functional and conformational crosstalk. *Mol. Cell* **75**, 1131–1146.e6 https://doi.org/10.1016/j.molcel.2019.07.022
79 Blaza, J.N., Serreli, R., Jones, A.J., Mohammed, K. and Hirst, J. (2014) Kinetic evidence against partitioning of the ubiquinone pool and the catalytic relevance of respiratory-chain supercomplexes. *Proc. Natl Acad. Sci. U.S.A.* **111**, 15735–15740 https://doi.org/10.1073/pnas.1413855111
80 Hirst, J. (2018) Open questions: respiratory chain supercomplexes—why are they there and what do they do? *BMC Biol.* **16**, 111 https://doi.org/10.1186/s12915-018-0577-5
81 Letts, J.A. and Sazanov, L.A. (2017) Clarifying the supercomplex: the higher-order organization of the mitochondrial electron transport chain. *Nat. Struct. Mol. Biol.* **24**, 800–808 https://doi.org/10.1038/nsmb.3460
82 Lobo-Jarne, T., Pérez-Pérez, R., Fontanesi, F., Timón-Gómez, A., Wittig, I., Peñas, A. et al. (2020) Multiple pathways coordinate assembly of human mitochondrial complex IV and stabilization of respiratory supercomplexes. *EMBO J.* **39**, e103912 https://doi.org/10.15252/embj.2019103912
83 Timón-Gómez, A., Garlich, J., Stuart, R.A., Ugalde, C. and Barrientos, A. (2020) Distinct roles of mitochondrial HIGD1A and HIGD2A in respiratory complex and supercomplex biogenesis. *Cell Rep.* **31**, 107607 https://doi.org/10.1016/j.celrep.2020.107607
84 Milenkovic, D., Misic, J., Hevler, J.F., Molinié, T., Chung, I., Atanassov, I. et al. (2023) Preserved respiratory chain capacity and physiology in mice with profoundly reduced levels of mitochondrial respirasomes. *Cell Metab* **35**, 1799–1813.e7 https://doi.org/10.1016/j.cmet.2023.07.015
85 Parmar, G., Fong-McMaster, C., Pileggi, C., Patten, D.A., Cuillerier, A., Myers, S. et al. (2024) Accessory subunit NDUFB4 participates in mitochondrial complex I supercomplex formation. *J. Biol. Chem.* **300**, 105626. https://doi.org/10.1016/j.jbc.2024.105626
86 Agip, A.-N.A., Chung, I., Sanchez-Martinez, A., Whitworth, A.J. and Hirst, J. (2023) Cryo-EM structures of mitochondrial respiratory complex I from *Drosophila melanogaster*. *eLife* **12**, e84424 https://doi.org/10.7554/eLife.84424
87 Brischigliaro, M., Cabrera-Orefice, A., Arnold, S., Viscomi, C., Zeviani, M. and Fernández-Vizarra, E. (2023) Structural rather than catalytic role for mitochondrial respiratory chain supercomplexes. *eLife* **12**, RP88084 https://doi.org/10.7554/eLife.88084.2
88 Ramirez-Aguilar, S.J., Keuthe, M., Rocha, M., Fedyaev, V.V., Kramp, K., Gupta, K.J. et al. (2011) The composition of plant mitochondrial supercomplexes changes with oxygen availability. *J. Biol. Chem.* **286**, 43045–43053 https://doi.org/10.1074/jbc.M111.252544